Contents lists available at ScienceDirect

Digital Chinese Medicine

journal homepage: http://www.keaipublishing.com/dcmed

Attenuation of oxidative injury in retinal photoreceptor cells by Gouqizi (Lycii Fructus) and Danshen (Salviae Miltiorrhizae Radix et Rhizoma) through modulation of ANGPTL4

Jun Peng[a], Junjiang Jiang[b], Junnan Zhong[b], Siyi Zhou[b], Tingyan Hu[b], Xuyu Chen[b], Qinghua Peng[c], Yasha Zhou[b*]

a. Department of Ophthalmology, The First Hospital of Hunan University of Chinese Medicine, Changsha, Hunan 410007, China

b. School of Integrated Chinese and Western Medicine, Hunan University of Chinese Medicine, Changsha, Hunan 410208, China

c. School of Traditional Chinese Medicine, Hunan University of Chinese Medicine, Changsha, Hunan 410208, China

ARTICLE INFO

Article history
Received 19 March 2026
Accepted 06 May 2026
Available online 25 June 2026

Keywords
Gouqizi (Lycii Fructus) and Danshen (Salviae Miltiorrhizae Radix et Rhizoma)
Retinal photoreceptor cells
Angiopoietin-like 4
Oxidative injury
Apoptosis

ABSTRACT

Objective To investigate the protective effects of Gouqizi (Lycii Fructus, GQZ)-Danshen (Salviae Miltiorrhizae Radix et Rhizoma, DS) against hydrogen peroxide (H_2O_2)-induced oxidative injury in 661W retinal photoreceptor cells and to explore whether these effects involve angiopoietin-like 4 (ANGPTL4).

Methods Liquid chromatography-mass spectrometry (LC-MS) was used to identify the major components of GQZ-DS aqueous extract. An H_2O_2-induced oxidative injury model was established in 661W cells. Working concentrations of H_2O_2 and GQZ-DS were determined using the cell counting kit-8 (CCK-8) assay. Cells were subjected to GQZ-DS, ANGPTL4 knockdown, or ANGPTL4 overexpression as indicated. Flow cytometry was used to analyze cell cycle distribution, apoptotic rate, and intracellular reactive oxygen species (ROS). Colorimetric determination of malondialdehyde (MDA) content and superoxide dismutase (SOD) activity using the thiobarbituric acid (TBA) method was performed. The protein expression level of ANGPTL4 was assessed by immunofluorescence. Reverse transcription-quantitative polymerase chain reaction (RT-qPCR) was performed to quantify the mRNA level of ANGPTL4. Western blot was used to detect the protein levels of ANGPTL4 and cleaved caspase-3.

Results LC-MS identified five major constituents in the GQZ-DS aqueous extract: 2-O-β-D-glucopyranosyl-L-ascorbic acid, rutin, D-galactose, salvianolic acid A, and tanshinone IIA. The CCK-8 method selected 300 μmol/L H_2O_2 as the oxidative stress condition for experiments, and 0.05 and 0.1 g/mL were selected as the low and high doses of GQZ-DS, respectively, for subsequent experiments. The intervention with H_2O_2 resulted in reduced cell viability, elevated ROS and MDA levels, decreased SOD activity, increased apoptotic rate, upregulated cleaved caspase-3 expression, and G0/G1 phase cell cycle arrest of 661W cells. Both low and high doses of GQZ-DS alleviated these alterations, with high dose exhibiting stronger protective effects ($P < 0.05$ or $P < 0.01$). GQZ-DS also downregulated ANGPTL4 expression at both the mRNA and protein levels. Following plasmid transfection of cells, the study further revealed that ANGPTL4 knockdown mitigated oxidative stress and apoptosis-related injury, whereas ANGPTL4 overexpression exacerbated these pathological changes. Moreover, GQZ-DS partially reversed the degree of cellular oxidative damage induced by ANGPTL4 overexpression.

*Corresponding author: Yasha Zhou, E-mail: yashazhou@hnucm.edu.cn.

Peer review under the responsibility of Hunan University of Chinese Medicine.

DOI: 10.1016/j.dcmed.2026.05.011

Citation: PENG J, JIANG JJ, ZHONG JN, et al. Attenuation of oxidative injury in retinal photoreceptor cells by Gouqizi (Lycii Fructus) and Danshen (Salviae Miltiorrhizae Radix et Rhizoma) through modulation of ANGPTL4. Digital Chinese Medicine, 2026, 9(2): 290-301.

Conclusion GQZ-DS can alleviate the H_2O_2-induced oxidative injury of 661W retinal photoreceptor cells, and the effects are related to the down-regulation of ANGPTL4 expression.

1 Introduction

Retinal photoreceptor cells are essential for visual signal transduction, and their dysfunction or loss constitutes a major pathological basis of irreversible visual impairment. In several common retinal disorders, including age-related macular degeneration, diabetic retinopathy, and retinitis pigmentosa, the initiating causes differ, yet progressive photoreceptor injury remains a shared pathological outcome. Due to their high oxygen consumption and membranes enriched in polyunsaturated fatty acids, photoreceptors are particularly susceptible to damage mediated by reactive oxygen species (ROS). Consequently, oxidative stress has been recognized as a critical driver of photoreceptor apoptosis and retinal degeneration [1]. Despite this, current therapeutic options for progressive photoreceptor loss remain limited. Available clinical approaches are largely supportive in nature—such as nutritional supplementation with vitamin A or lutein-and are insufficient to effectively halt disease progression [2].

In traditional Chinese medicine (TCM), retinal degenerative disorders are commonly conceptualized as conditions involving both deficiency in origin and blood stasis in manifestation. Based on this framework, therapeutic strategies that combine tonifying deficiency with promoting blood circulation have been widely applied in clinical practice. Gouqizi (Lycii Fructus, GQZ)-Danshen (Salviae Miltiorrhizae Radix et Rhizoma, DS) constitute a representative herb pair derived from this therapeutic rationale and are frequently used in the treatment of retinal degenerative diseases, and the combination of GQZ-DS exhibited pronounced therapeutic benefits [3-5]. GQZ has been reported to exert anti-inflammatory, antioxidant, and neuroprotective effects through multiple targets and pathways [6, 7], whereas DS has been shown to reduce ROS accumulation, enhance superoxide dismutase (SOD) activity, and alleviate oxidative stress [8]. Collectively, these observations support the possibility that GQZ-DS may protect retinal cells under oxidative stress conditions.

Angiopoietin-like 4 (ANGPTL4) is a multifunctional secreted protein involved in angiogenesis, inflammation, oxidative stress, and metabolic regulation [9, 10]. In ocular research, ANGPTL4 has been studied mainly in the context of stress-related retinal diseases such as diabetic retinopathy, age-related macular degeneration, and retinal vein occlusion [11, 12]. Elevated ANGPTL4 expression in these conditions has been associated with pathological retinal remodeling and disease progression. Although direct evidence linking ANGPTL4 to photoreceptor oxidative injury remains limited, its documented involvement in retinal stress-related processes makes it a plausible candidate mediator in the present setting.

In the present study, we established an hydrogen peroxide (H_2O_2)-induced oxidative injury model in 661W retinal photoreceptor cells and combined it with ANGPTL4 knockdown and overexpression approaches to investigate the protective effects of GQZ-DS. We further examined whether the observed effects were associated with alterations in ANGPTL4 expression. This study aimed to provide experimental evidence for the protective effects of GQZ-DS against photoreceptor oxidative injury and to explore a possible mechanistic framework for its action.

2 Materials and methods

2.1 Cell culture

Mouse 661W retinal photoreceptor cells, provided by the Eye Institute of Xiamen University, were cultured in Dulbecco's Modified Eagle medium (DMEM) supplemented with 10% fetal bovine serum (FBS), 1% penicillin-streptomycin, and Cellmaxin at 37 °C in a humidified incubator containing 5% CO_2. Cells were used at passage 10.

2.2 Reagents and instruments

GQZ (Ningxia Zhongning Goji Industry Development Co., Ltd, China) and DS (Shandong Baicheng Traditional Chinese Medicine Decoction Pieces Co., Ltd., China) were authenticated by Professor Zhiying Yuan in Hunan University of Chinese Medicine. The following reagents were obtained from the indicated sources: H_2O_2 (Sigma-Aldrich, Germany); Annexin V-allophycocyanin (APC)/propidium iodide (PI) apoptosis detection kit (Jiangsu Keygen Biotech Corp., Ltd., China); N-acetyl-L-cysteine (NAC; Shanghai Zeye Biotechnology Co., Ltd., China); shRNA plasmid and overexpression plasmid (Wuhan Hualianke Biotechnology Co., Ltd., China); mRNA reverse transcription kit (Beijing Comwin Biotech Co., Ltd., China); ROS assay kit (Shanghai Beyotime Biotechnology Co., Ltd., China); malondialdehyde (MDA) kit (Nanjing Jiancheng Technology Co., Ltd., China); cell counting kit-8 (CCK-8) and SOD detection kit (Changsha Abbiwell Biotechnology Co., Ltd., China); β-actin antibody (1 : 5 000), Dylight 680 goat anti mouse IgG (1 : 10 000), Dylight 800, goat anti rabbit IgG (1 : 10 000), and total protein extraction kit (Immunoway Corporation, USA);

ANGPTL4 antibody (Hunan Aifang Biotechnology Co., Ltd., China; 1 : 1 000) and cleaved caspase-3 antibody (Affinity Biosciences, China; 1 : 1 000).

The following instruments were used: flow cytometer (Beckman Coulter Inc., A00-1-1102); reverse transcription-quantitative polymerase chain reaction (RT-qPCR) instrument (Applied Biosystems, QuantStudio 1); ultra-high performance liquid chromatograph (Thermo Fisher Scientific, Vanquish); high-resolution mass spectrometer (Thermo Fisher Scientific, Orbitrap Exploris 120); and fluorescence imaging system (Licor Corporation, Odyssey).

2.3 Preparation and chemical characterization of GQZ-DS extract

GQZ (15 g) and DS (15 g) were mixed [13], and the mixture was decocted twice with boiling distilled water. The aqueous extract was centrifuged at 10 000 rpm for 30 min. The resulting decoction was sequentially concentrated and freeze-dried before storage at – 20 °C. The GQZ-DS extract was sterilized by filtering through a 0.22-μm filter membrane.

To characterize the major constituents of the GQZ-DS aqueous extract, liquid chromatography-mass spectrometry (LC-MS) analysis was performed in both positive and negative ion modes. The aqueous extract was mixed with 1 000 μL of extraction solvent containing an isotope-labeled internal standard (methanol/acetonitrile/water, 2 : 2 : 1, v/v/v). The mixture was vortexed for 30 s, sonicated in an ice-water bath for 5 min, and then incubated at – 20 °C for 1 h. After centrifugation at 12 000 rpm for 15 min, the supernatant was collected and filtered through a 0.22-μm membrane before analysis.

Chromatographic separation was carried out using a Phenomenex Kinetex C18 column (100 mm × 2.1 mm, 2.6 μm particle size). The mobile phase consisted of solvent A (water containing 0.01% acetic acid) and solvent B (isopropanol/acetonitrile, 1 : 1, v/v). The autosampler temperature was maintained at 4 °C, and the injection volume was 2 μL. Mass spectrometric data were acquired using an Orbitrap Exploris 120 high-resolution mass spectrometer controlled by Xcalibur 4.4 software. The electrospray ionization (ESI) source parameters were set as follows: sheath gas flow rate, 50 Arb; auxiliary gas flow rate, 15 Arb; capillary temperature, 320 °C; full MS resolution, 60 000; MS/MS resolution, 15 000; stepped normalized collision energy, 20%, 30%, and 40%; and spray voltage, 3.8 kV in positive ion mode and – 3.4 kV in negative ion mode. Metabolite identification was performed using an R package and the BiotreeDB (V3.0) database. The results are presented as total ion chromatograms (TIC).

2.4 Cell viability assay and concentration screening

2.4.1 Screening of H_2O_2 concentration Log-phase 661W cells were harvested, resuspended, and seeded into 96-well plates at a density of 1×10^5 cells/mL, with 100 μL of cell suspension added to each well. After cell attachment, the culture medium was replaced with fresh medium containing H_2O_2 at final concentrations of 50, 100, 200, or 300 μmol/L, respectively. Cells were then exposed to H_2O_2 for 15 min to induce oxidative stress. Cells in the blank group were maintained in the absence of H_2O_2. Subsequently, 100 μL of medium containing 10% CCK-8 reagent was added to each well, and the cells were incubated at 37 °C for 4 h in the dark. Absorbance was measured at 450 nm using a microplate reader, and relative cell viability was calculated using the following formula: cell viability (%) = $[(OD_{sample} - OD_{no\ cells})/(OD_{blank} - OD_{no\ cells})] \times 100\%$.

2.4.2 Screening of GQZ-DS concentrations To determine the appropriate working concentrations of GQZ-DS for subsequent experiments, 661W cells were initially seeded into 96-well plates and divided into five groups: blank group, model group, and GQZ-DS aqueous extract treatment groups at concentrations of 0.025, 0.05, and 0.1 g/mL, respectively. Cells in the treatment groups were pretreated with the respective concentrations of GQZ-DS for 24 h. Thereafter, all groups except the blank group were exposed to H_2O_2 to induce oxidative cellular injury. Finally, cells were incubated with fresh medium containing 10% CCK-8 reagent at 37 °C for 4 h in the dark. Absorbance at 450 nm was then measured using a microplate reader. Relative cell viability was calculated to identify suitable GQZ-DS concentrations for subsequent experiments.

2.5 Cell culture and intervention

2.5.1 GQZ-DS treatment in the H_2O_2-induced 661W cell model 661W cells were seeded and divided into five experimental groups: blank-1, model-1, GQZ-DS low-dose (GQZ-DS-LD), GQZ-DS high-dose-1 (GQZ-DS-HD-1), and positive control. Cells in the GQZ-DS-LD, GQZ-DS-HD-1, and positive control groups were pretreated for 4 h with 0.05 g/mL GQZ-DS, 0.1 g/mL GQZ-DS, or 100 μmol/L NAC, respectively. Following pretreatment, oxidative injury was induced in the model-1 and all treatment groups by exposure to 300 μmol/L H_2O_2 for 15 min, whereas cells in the blank-1 group received fresh culture medium only. Subsequently, cell cycle distribution and intracellular ROS levels were assessed using flow cytometry. MDA content and SOD activity were measured using the thiobarbituric acid (TBA) colorimetric method. The mRNA expression level of ANGPTL4 was measured by RT-qPCR, and the protein expression level of ANGPTL4 was assessed by immunofluorescence.

2.5.2 ANGPTL4 knockdown and overexpression in the H_2O_2-induced 661W cell model To investigate the role of ANGPTL4 in oxidative stress, 661W cells were assigned into six groups: shRNA negative control (sh-NC), empty

vector-1 (EV-1), ANGPTL4 knockdown-1 (ANGPTL4-KD-1), ANGPTL4-KD-2, ANGPTL4-KD-3, and ANGPTL4 overexpression-1 (ANGPTL4-OE-1). Cells in all groups were transfected with the respective plasmids and cultured for 48 h to establish gene knockdown or overexpression. After transfection, all groups were subjected to 300 μmol/L H_2O_2 for 15 min to induce oxidative injury. Transfection efficiency was subsequently confirmed by RT-qPCR and Western blot.

2.5.3 GQZ-DS treatment combined with ANGPTL4 manipulation in the H_2O_2-induced 661W cell model To determine whether the protective effects of GQZ-DS involve alterations in ANGPTL4, cells were divided into five groups: blank-2, ANGPTL4-OE-2, ANGPTL4-KD-3, GQZ-DS-HD-2, and model-2. Cells in the GQZ-DS-HD-2 group were pretreated with 0.1 g/mL GQZ-DS for 4 h, while those in the ANGPTL4-OE-2 and ANGPTL4-KD-3 groups underwent plasmid transfection as described above. Subsequently, except for the blank-2 group, all groups were exposed to 300 μmol/L H_2O_2 for 15 min to induce oxidative injury. Then the apoptotic rate was measured by flow cytometry, and the protein expression levels of cleaved caspase-3 were examined by Western blot.

2.5.4 GQZ-DS treatment in ANGPTL4-knockdown and ANGPTL4-overexpressing 661W cells under oxidative stress To further evaluate whether ANGPTL4 is required for the protective action of GQZ-DS, cells were allocated into six groups: EV-2, ANGPTL4-KD-3, ANGPTL4-OE-3, EV-2 + GQZ-DS-HD, ANGPTL4-KD-3 + GQZ-DS-HD, and ANGPTL4-OE-3 + GQZ-DS-HD. After 48 h of transfection, cells in the GQZ-DS-treated groups were pretreated with 0.1 g/mL GQZ-DS for 4 h, followed by exposure to 300 μmol/L H_2O_2 for 15 min. The corresponding non-GQZ-DS groups underwent the same H_2O_2 exposure without GQZ-DS pretreatment. Cell cycle distribution, apoptotic rate, and intracellular ROS levels were analyzed by flow cytometry, and MDA content and SOD activity were measured using the TBA colorimetric method.

2.6 Flow cytometry analysis

2.6.1 Cell cycle distribution analysis by PI staining Harvest the cultured cells without excessive trypsinization and wash twice with cold phosphate buffered saline (PBS). Cells were then fixed by the addition of prechilled 75% ethanol and stored overnight at 4 °C. The fixed cells were washed twice with cold PBS to remove residual ethanol. After mixing well, 1 μg/mL PI staining solution was added, and the cells were incubated at 4 °C for 30 min in the dark. Cell cycle distribution was analyzed using flow cytometry. A total of 10 000 events was collected per sample. The percentages of cells in G0/G1, S, and G2/M phases were calculated using appropriate gating to exclude debris and cell aggregates.

2.6.2 Cell apoptosis detection analysis by annexin V-APC/PI staining Harvest the cultured cells with trypsin without ethylenediaminetetraacetic acid (EDTA). Wash the cells twice with PBS, centrifuge at 1 000 rpm for 5 min each time, and collect approximately 7.2×10^5 cells. After adding 500 μL of binding buffer to suspend the cells, 100 μL aliquot of cell suspension was stained with 5 μL of annexin V-APC and 5 μL of PI at room temperature for 15 min in the dark. Samples were immediately analyzed by flow cytometry and the apoptotic rates were calculated.

2.6.3 Intracellular ROS detection by 2',7'-dichlorodihydrofluorescein diacetate (DCFH-DA) staining After the indicated treatments, cells were incubated with DCFH-DA at a final concentration of 10 μmol/L for 20 min at 37 °C in the dark. Cells were then washed with serum-free medium, harvested by trypsinization, and resuspended in PBS. Intracellular ROS fluorescence intensity was measured by flow cytometry, and the relative ROS level in each group was quantified.

2.7 Determination of MDA content and SOD activity

MDA content and SOD activity were determined using TBA colorimetric assay kits. Briefly, cells were collected and lysed, and the supernatants were obtained by centrifugation. Total protein concentration was measured using a bicinchoninic acid assay (BCA) protein assay for normalization. For the MDA assay, 500 μL of sample supernatant or MDA standard was mixed with 100 μL of TBA working solution in a 1.5 mL Eppendorf (EP) tube. The mixture was vortexed for 10 s and incubated in a boiling water bath at 95 °C for 40 min. The reaction was then quenched on ice for 10 min, followed by centrifugation at 3 000 rpm for 10 min at room temperature. The absorbance of the clear pink supernatant was measured at 532 nm, and MDA concentration was calculated from the standard curve. SOD activity was assessed using an inhibition-based colorimetric assay. Control, control blank, sample, and sample blank wells were prepared according to the kit protocol. After incubation at 37 °C for 20 min protected from light, absorbance was measured at 532 nm or 450 nm. The inhibition rate was calculated after background correction, and SOD activity was normalized to total protein concentration. MDA content was expressed as nmol/mg protein, and SOD activity was expressed as U/mg protein.

2.8 RT-qPCR analysis

Total RNA was extracted from 661W cells using TRIzol reagent according to the manufacturer's protocol. The extracted RNA was then reverse-transcribed into complementary DNA (cDNA) using a reverse transcription kit. Quantitative PCR was performed on a real-time PCR system using SYBR Green chemistry. The thermal cycling

conditions were as follows: initial denaturation at 95 °C for 10 min, followed by 40 cycles of 95 °C for 15 s and 60 °C for 30 s. *β-Actin* served as the internal reference gene. The relative mRNA expression level of *ANGPTL4* was calculated using the $2^{-\Delta\Delta Ct}$ method. All primer sequences used in this study are listed in Table 1.

Table 1 Primer sequences of target genes for RT-qPCR

Gene symbol	Primer sequence (5′→3′)	Length (bp)
ANGPTL4	F: TTCCACTCTATCCCACGGCAAC R: CAAATCTCAGGGCCACAACCAA	198
β-Actin	F: ACATCCGTAAAGACCTCTATGCC Reverse: TACTCCTGCTTGCTGATCCA	223

F, foward. R, reverse.

2.9 Immunofluorescence staining

Cells were washed three times with PBS and then fixed with 4% paraformaldehyde for 15 min at room temperature. Subsequently, the cells were permeabilized with 0.3% Triton X-100, blocked with 5% bovine serum albumin (BSA), and incubated overnight at 4 °C with ANGPTL4 antibody. After washing, the cells were incubated with the appropriate fluorescently conjugated secondary antibody in the dark, followed by counterstaining with DAPI for nuclear visualization. Images were captured using a fluorescence microscope, and fluorescence intensity was quantified using ImageJ software.

2.10 Western blot analysis

Total protein was extracted from cells using a protein extraction kit, and protein concentration was determined using the bicinchoninic acid (BCA) method. Equal amounts of protein were mixed with loading buffer, denatured at 100 °C for 5 min, separated by sodium dodecyl sulfate-polyacrylamide gel electrophoresis (SDS-PAGE), and transferred onto nitrocellulose membranes. The membranes were then blocked with 5% skim milk for 2 h at room temperature and incubated overnight at 4 °C with ANGPTL4, cleaved caspase-3, and β-actin antibodies. After washing with Tris-buffered saline containing Tween 20 (TBST), the membranes were incubated with the appropriate fluorescently conjugated secondary antibodies for 90 min at room temperature in the dark. Protein bands were visualized using a fluorescence imaging system, and band intensities were quantified using Image Studio, with β-actin serving as the loading control.

2.11 Statistical analysis

Statistical analyses were performed using SPSS version 27.0. Data are presented as mean ± standard deviation (SD). Normality and homogeneity of variance were assessed before group comparisons. For comparisons between two groups, an independent-samples *t* test was used when the data met parametric assumptions; otherwise, the Mann-Whitney *U* test was applied. For comparisons among multiple groups, one-way analysis of variance (ANOVA) or the corresponding nonparametric test (Kruskal-Wallis test) was applied. $P < 0.05$ was considered statistically significant.

3 Results

3.1 Major compounds of GQZ-DS aqueous extract

TIC analysis revealed five major compounds in the GQZ-DS aqueous extract: 2-O-β-D-glucopyranosyl-L-ascorbic acid (45.2 s), rutin (291.6 s), D-galactose (41.9 s), salvianolic acid A (302.5 s), and tanshinone IIA (485.9 s). These findings indicated that the extract contained the principal detectable components of GQZ-DS. The positive- and negative-ion TIC profiles are presented in Figure 1, and the identified compounds are summarized in Table 2.

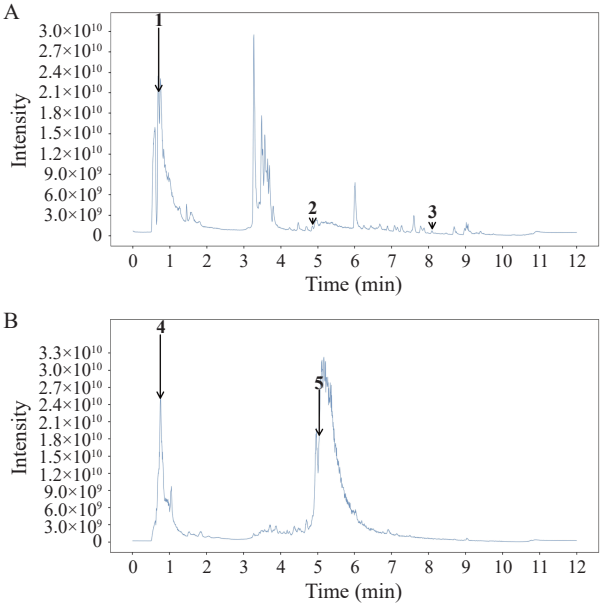

Figure 1 TIC of GQZ-DS aqueous extract

A, positive-ion TIC of GQZ-DS. Peaks: **1**, D-galactose; **2**, rutin; **3**, tanshinone IIA. B, negative-ion TIC of GQZ-DS. Peaks: **4**, 2-O-β-D-glucopyranosyl-L-ascorbic acid; **5**, salvianolic acid A.

3.2 Establishment of the oxidative injury model and selection of GQZ-DS concentrations

Exposure to H_2O_2 induced oxidative injury in 661W cells. No significant differences in cell viability were observed between the blank group and the groups treated with 50, 100, or 200 μmol/L H_2O_2 ($P > 0.05$). In contrast, treatment with 300 μmol/L H_2O_2 significantly reduced relative cell viability ($P < 0.01$). Based on these results, exposure to 300 μmol/L H_2O_2 for 15 min was selected as the oxidative stress condition for subsequent experiments (Figure 2A).

Table 2 Main chemical compounds identified in the GQZ-DS aqueous extract

Compound	Molecular formula	m/z	Retention time (s)
2-O-β-D-glucopyranosyl-L-ascorbic acid	$C_{12}H_{18}O_{11}$	337.076 8	45.2
Rutin	$C_{27}H_{30}O_{16}$	611.1590	291.6
D-galactose	$C_6H_{12}O_6$	203.052 2	41.9
Salvianolic acid A	$C_{26}H_{22}O_{10}$	493.112 8	302.5
Tanshinone IIA	$C_{19}H_{18}O_3$	295.131 9	485.9

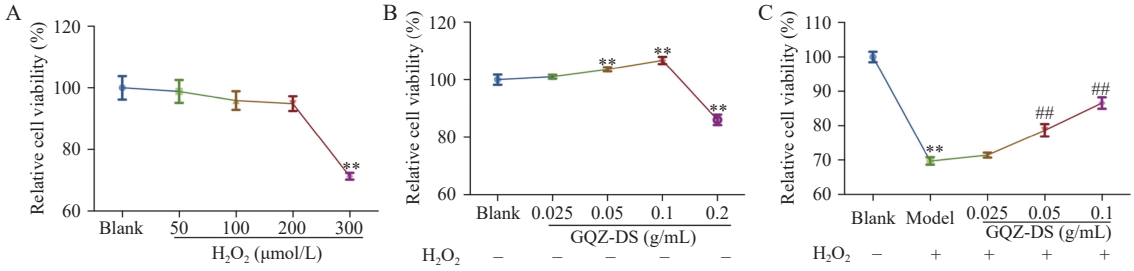

Figure 2 Screening of H_2O_2 and GQZ-DS concentrations using CCK-8 assay

A, relative cell viability of 661W cells treated with different concentrations of H_2O_2. B and C, relative cell viability of 661W cells cultured without H_2O_2 or with H_2O_2, respectively. $^{**}P < 0.01$, compared with blank group. $^{\#\#}P < 0.01$, compared with model group.

In the absence of H_2O_2, treatment with GQZ-DS at concentrations of 0.05 and 0.1 g/mL significantly increased relative cell viability compared with the blank group, whereas 0.2 g/mL GQZ-DS reduced cell viability ($P < 0.01$). Under oxidative stress induced by 300 μmol/L H_2O_2, cell viability in the model group was significantly lower than that in the blank group ($P < 0.01$). Compared with the model group, GQZ-DS at 0.1 g/mL exerted the strongest protective effects, followed by 0.05 g/mL ($P < 0.01$). Therefore, 0.05 and 0.1 g/mL were selected as the low and high doses of GQZ-DS, respectively, for subsequent experiments (Figure 2B and 2C).

3.3 Attenuation of oxidative injury in 661W cells by GQZ-DS

Cell cycle analysis revealed that, compared with the blank-1 group, the model-1 group exhibited a significantly higher proportion of cells in the G0/G1 phase ($P < 0.01$), indicating H_2O_2-induced cell cycle arrest and impaired proliferative activity. Compared with the model-1 group, the GQZ-DS-LD, GQZ-DS-HD-1, and positive control groups all showed a reduced proportion of cells in G0/G1 (all $P < 0.01$), suggesting that GQZ-DS alleviated oxidative stress-related cell cycle disturbance. The effects were more pronounced in the GQZ-DS-HD-1 group than in the GQZ-DS-LD group ($P < 0.01$) (Figure 3A and 3B).

Consistent with these findings, oxidative stress markedly increased intracellular ROS and MDA levels and decreased SOD activity in the model-1 group relative to the blank-1 group ($P < 0.01$). GQZ-DS significantly reduced ROS and MDA levels and increased SOD activity compared with the model-1 group ($P < 0.01$ or $P < 0.05$). The protective effects were stronger in the GQZ-DS-HD-1 group than in the GQZ-DS-LD group ($P < 0.01$). Collectively, these results demonstrate that GQZ-DS effectively attenuated H_2O_2-induced oxidative damage in 661W cells (Figure 3C – 3F).

3.4 Reduction of ANGPTL4 expression in oxidatively injured 661W cells by GQZ-DS

Immunofluorescence analysis showed that ANGPTL4 protein expression was markedly increased in the model-1 group compared with the blank-1 group ($P < 0.01$), whereas GQZ-DS significantly reduced ANGPTL4 fluorescence intensity ($P < 0.01$). The reduction was more pronounced in the GQZ-DS-HD-1 group than in the GQZ-DS-LD group ($P < 0.05$) (Figure 4A and 4B).

Consistent with these findings, RT-qPCR analysis showed a similar overall trend. Compared with the blank-1 group, ANGPTL4 mRNA expression level was significantly upregulated in the model-1 group ($P < 0.01$). Both GQZ-DS-LD and GQZ-DS-HD-1 significantly reduced ANGPTL4 mRNA expression level ($P < 0.01$), with a greater suppression observed in the GQZ-DS-HD-1 group ($P < 0.01$) (Figure 4C). Taken together, these data indicate that the protective effects of GQZ-DS was associated with reduced ANGPTL4 expression in oxidatively injured 661W cells.

3.5 Effects of knockdown or overexpression of ANGPTL4 on oxidative injury

Among the three knockdown constructs tested, ANGPTL4-KD-3 exhibited the strongest reduction in ANGPTL4 mRNA expression level ($P < 0.01$) and was therefore selected

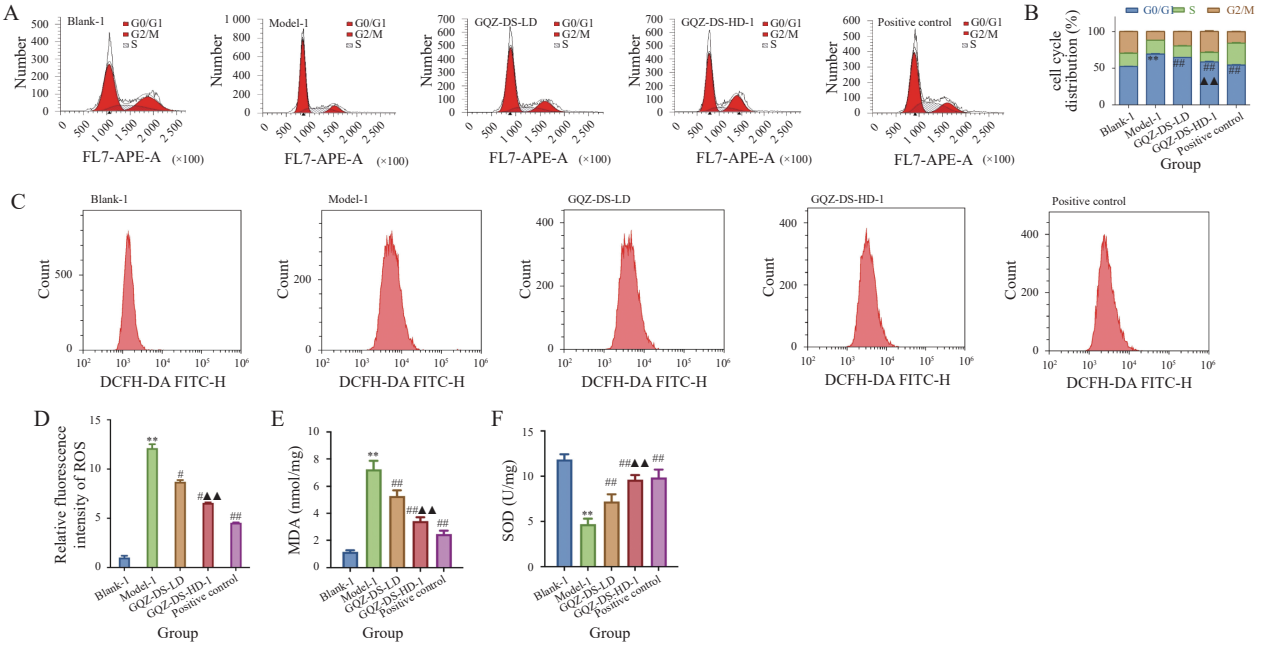

Figure 3 Cell cycle distribution and levels of ROS, MDA, and SOD in different groups

A, flow cytometric histogram of cell cycle. B, quantitative comparison of cell cycle distribution. C, flow cytometric histograms of intracellular ROS levels in different groups. D – F, levels of ROS, MDA, and SOD, respectively. $^{**}P < 0.01$, compared with blank-1 group. $^{\#}P < 0.05$ and $^{\#\#}P < 0.01$, compared with model-1 group. $^{\blacktriangle\blacktriangle}P < 0.01$, compared with GQZ-DS-LD group.

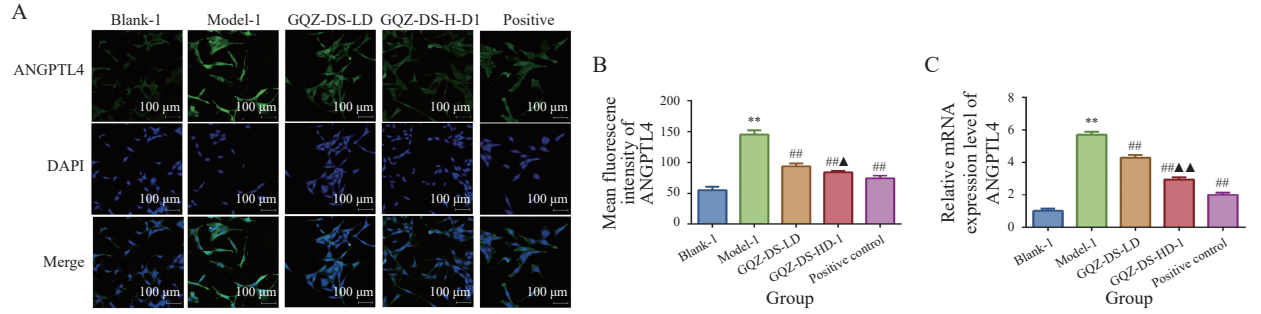

Figure 4 Protein and mRNA expression levels of ANGPTL4 of 661W cells in different groups

A, immunofluorescence staining of ANGPTL4 in 661W cells. B, quantitative analysis of ANGPTL4 protein expression level in different groups. C, relative mRNA expression level of ANGPTL4 in 661W cells. $^{**}P < 0.01$, compared with blank-1 group. $^{\#\#}P < 0.01$, compared with model-1 group. $^{\blacktriangle}P < 0.05$ and $^{\blacktriangle\blacktriangle}P < 0.01$, compared with GQZ-DS-LD group.

for subsequent experiments. Compared with the EV-1 group, ANGPTL4 mRNA expression level was significantly decreased in the ANGPTL4-KD-3 group ($P < 0.01$) and significantly increased in the ANGPTL4-OE-1 group ($P < 0.01$) (Figure 5A). Consistent changes were observed at the protein level by Western blot, confirming successful modulation of ANGPTL4 expression (Figure 5B and 5C).

ANGPTL4 influenced oxidative stress-related phenotypes in 661W cells. Compared with the ANGPTL4-KD-3 group, the ANGPTL4-OE-1 group exhibited higher levels of ROS and MDA and lower SOD activity ($P < 0.01$). These findings indicate that ANGPTL4 overexpression aggravated oxidative injury, whereas ANGPTL4 knockdown alleviated it. Thus, ANGPTL4 appears to play a functional role in the oxidative stress response of 661W cells (Figure 5D – 5G).

3.6 Reduction of ANGPTL4 expression and attenuation of apoptosis in oxidative injury of 661W cells by GQZ-DS

Compared with blank-2 group, the apoptotic rate and the protein expression levels of ANGPTL4 and cleaved caspase-3 were significantly increased in model-2 group ($P < 0.01$). In contrast, both GQZ-DS treatment and ANGPTL4 knockdown partially reversed these alterations ($P < 0.01$ or $P < 0.05$). Compared with ANGPTL4-OE-2 group, both the GQZ-DS-HD-2 and ANGPTL4-KD-3 group exhibited reduction in the apoptotic rate and protein expression of ANGPTL4 and cleaved caspase-3 ($P < 0.01$) (Figure 6A – 6E).

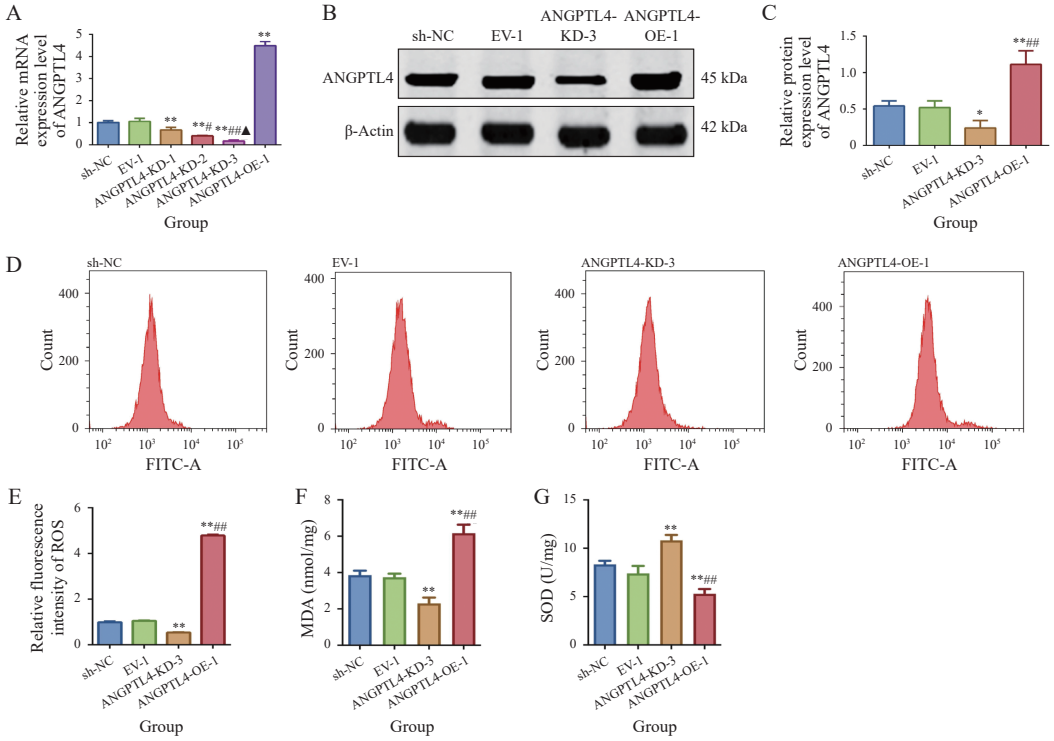

Figure 5 Protein and mRNA expression level of ANGPTL4 and levels of ROS, MDA, and SOD of 661W cells in different groups

A, relative mRNA expression of ANGPTL4 in different groups. $^{**}P < 0.01$, compared with EV-1 group. $^{\#}P < 0.05$ and $^{\#\#}P < 0.01$, compared with ANGPTL4-KD-1 group. $^{\blacktriangle}P < 0.05$, compared with ANGPTL4-KD-2 group. B, protein bands of ANGPTL4 detected by Western blot. C, relative protein expression level of ANGPTL4 in different groups. $^{*}P < 0.05$ and $^{**}P < 0.01$, compared with EV-1 group. $^{\#\#}P < 0.01$, compared with ANGPTL4-KD-3 group. D, flow cytometric histograms of intracellular ROS levels in different groups. E – G, levels of ROS, MDA, and SOD in different groups, respectively. $^{**}P < 0.01$, compared with EV-1 group. $^{\#\#}P < 0.01$, compared with ANGPTL4-KD-3 group.

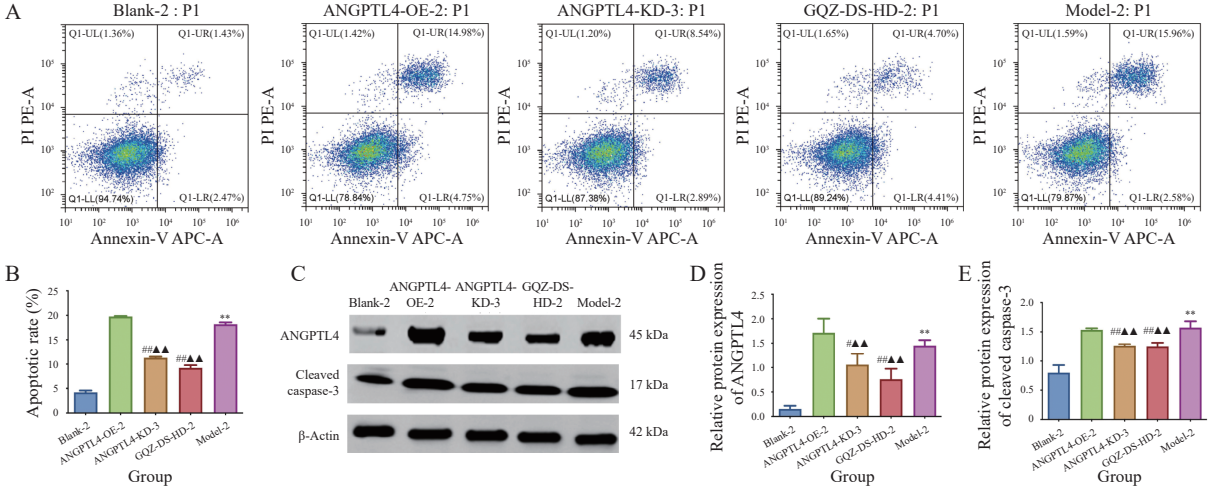

Figure 6 Apoptotic rate and protein expression levels of ANGPTL4 and cleaved caspase-3 in 661W cells

A, annexin V-APC/PI dot plots of apoptosis detected by flow cytometry. B, quantitative analysis of apoptotic rates. C, representative protein bands of ANGPTL4 and cleaved caspase-3. D and E, relative protein expression levels of ANGPTL4 and cleaved caspase-3, respectively. $^{**}P < 0.01$, compared with blank-2 group. $^{\#}P < 0.05$ and $^{\#\#}P < 0.01$, compared with model-2 group. $^{\blacktriangle\blacktriangle}P < 0.01$, compared with ANGPTL4-OE-2 group.

3.7 Partial alleviation of oxidative injury by GQZ-DS under ANGPTL4 modulation

Compared with the EV-2 group, both the EV-2 + GQZ-DS-HD and the ANGPTL4-KD-3 groups showed improved cellular status, reflected by lower ROS and MDA levels, higher SOD activity, and altered cell cycle distribution ($P < 0.01$). In contrast, ANGPTL4 overexpression (ANGPTL4-OE-3 group) aggravated oxidative injury and was associated with higher ROS and MDA levels and lower SOD activity, ($P < 0.01$) (Figure 7A – 7F).

Compared with the ANGPTL4-OE-3 group, the

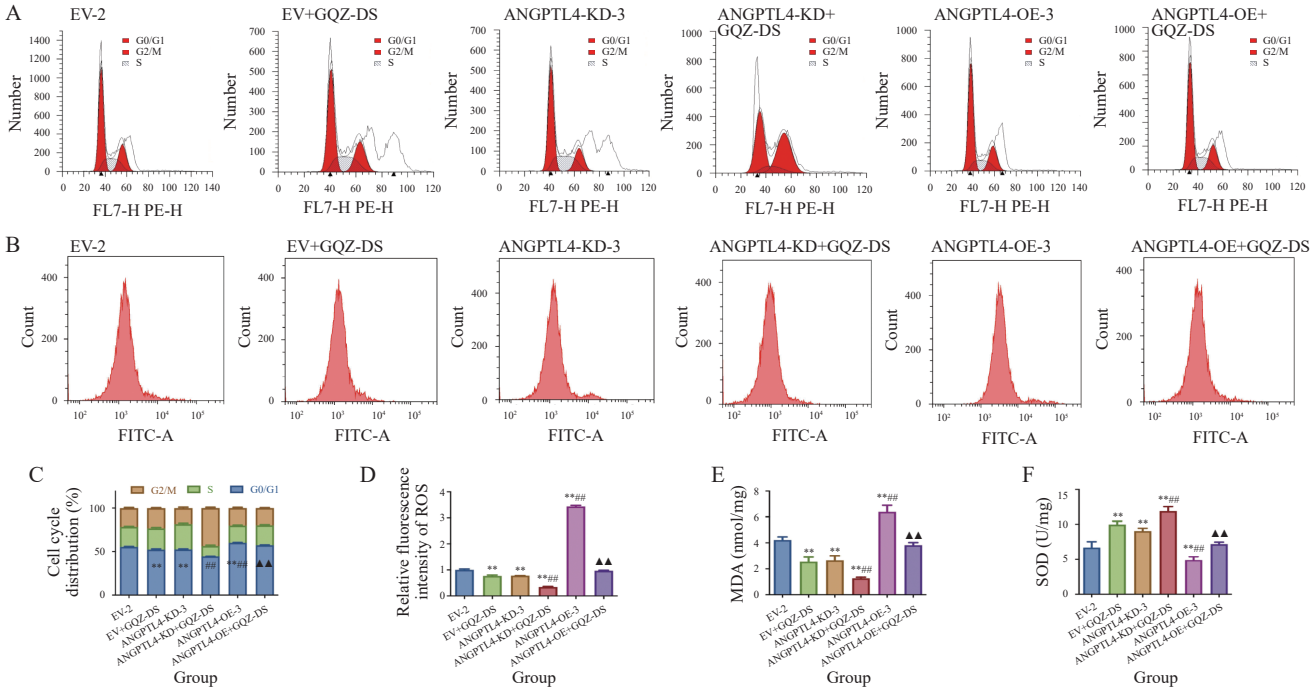

Figure 7 Cell cycle distribution and levels of ROS, MDA, and SOD in different groups

A, flow cytometric histogram of cell cycle distribution. B, flow cytometric histograms of intracellular ROS levels. C, quantitative comparison of cell cycle distribution. D – F, levels of ROS, MDA, and SOD, respectively. $^{**}P < 0.01$, compared with EV-2 group. $^{\#\#}P < 0.01$, compared with ANGPTL4-KD-3 group. $^{\blacktriangle\blacktriangle}P < 0.01$, compared with ANGPTL4-OE-3 group.

ANGPTL4-OE-3 + GQZ-DS-HD group exhibited reduced ROS and MDA levels, increased SOD activity, and partial correction of cell cycle abnormalities ($P < 0.01$), indicating that GQZ-DS could at least partially counteract the adverse effects of ANGPTL4 overexpression. Furthermore, compared with the ANGPTL4-KD-3 group, the ANGPTL4-KD-3 + GQZ-DS-HD group showed further reductions in oxidative stress markers and a further increase in SOD activity ($P < 0.01$), suggesting that the protective effects of GQZ-DS was associated with ANGPTL4 knockdown.

4 Discussion

In this study, we established an H_2O_2-induced oxidative injury model in 661W retinal photoreceptor cells and found that oxidative stress markedly reduced cell viability, increased ROS and MDA accumulation, decreased SOD activity, induced G0/G1 phase arrest, and promoted apoptosis. GQZ-DS significantly alleviated these oxidative injury-related changes and was accompanied by reduced ANGPTL4 expression at both the mRNA and protein levels. Further functional experiments showed that ANGPTL4 knockdown attenuated oxidative stress and apoptosis, whereas ANGPTL4 overexpression aggravated these alterations. Importantly, GQZ-DS partially counteracted the pro-injury effects caused by ANGPTL4 overexpression, suggesting that suppression of ANGPTL4 is involved in the protective action of GQZ-DS against oxidative damage in 661W cells.

4.1 Oxidative stress in degenerative diseases of RPC and the potential role of ANGPTL4

Oxidative stress plays a well-established role in the onset and progression of retinal degenerative diseases. In the present study, exposure to H_2O_2 induced a typical oxidative injury phenotype in 661W retinal photoreceptor cells, as evidenced by increased ROS and MDA levels, decreased SOD activity, and G0/G1 phase cell cycle arrest. Collectively, these findings indicate that oxidative stress disrupts intracellular redox homeostasis and impairs normal cellular function. Notably, pretreatment with GQZ-DS significantly reduced ROS and MDA accumulation, restored SOD activity, and alleviated G0/G1 phase arrest, suggesting that GQZ-DS exerts a protective effect against oxidative injury in retinal photoreceptor cells.

ANGPTL4 is a multifunctional secreted protein involved in oxidative stress, inflammation, lipid metabolism, and tissue remodeling. Previous studies have shown that oxidative stress can activate inflammatory pathways, while excessive inflammatory responses may in turn aggravate oxidative injury, thereby establishing a self-amplifying pathological cycle [14, 15]. In metabolic diseases such as diabetes and obesity, persistent upregulation of ANGPTL4 inhibits tissue fatty acid uptake, promotes ectopic lipid deposition, and enhances mitochondrial ROS production, ultimately exacerbating oxidative stress [16-18]. These findings suggest that pathologically elevated ANGPTL4 may act not merely as a passive biomarker, but as an active driver that indirectly fuels oxidative damage

and disease progression. Retinal degenerative diseases are closely associated with hypoxia and oxidative stress [19, 20]. Hypoxic stress further impairs mitochondrial function, increases ROS generation, and aggravates cellular damage. Within this context, ANGPTL4 emerges as a biologically plausible stress-responsive factor implicated in retinal injury.

4.2 Physiological correlation between ANGPTL4 and degenerative diseases of retinal photoreceptor cells

As a specialized neuronal cell type in the retina, retinal photoreceptor cells are highly vulnerable to oxidative stress and readily undergo apoptosis and functional impairment following injury [21, 22]. In ocular disorders, increased ANGPTL4 expression has been detected in the serum of patients with diabetic macular edema, as well as in the aqueous humor of patients with neovascular glaucoma and retinal vein occlusion [23-25]. These observations indicate that ANGPTL4 is associated with the progression and prognosis of various eye diseases. More importantly, WANG et al. [26] used single-cell RNA sequencing to analyze capillary–photoreceptor communication in diabetic retinopathy and found that ANGPTL4 participated in ligand-receptor interactions between retinal capillaries and photoreceptor cells. Knockdown of ANGPTL4 reduced apoptosis of both vascular endothelial cells and photoreceptor cells during disease progression, and retinal function improved as ANGPTL4-related signaling decreased, supporting a functional connection between ANGPTL4 and retinal photoreceptor cells. In the present study, ANGPTL4 expression increased following oxidative stress induction and decreased after GQZ-DS treatment. ANGPTL4 knockdown alleviated oxidative injury, whereas ANGPTL4 overexpression exacerbated it. Collectively, these findings suggest that ANGPTL4 is functionally relevant to oxidative damage of retinal photoreceptor cells.

Caspase-3 is an apoptotic execution marker, providing protein-level evidence of apoptosis. Cell cycle arrest is a recognized feature of pathological cellular senescence and proliferative dysfunction. WEN et al. [27] demonstrated that, in cardiomyocyte senescence induced by type 2 diabetes, knockdown of ANGPTL4 reduced senescence, whereas ANGPTL4 overexpression aggravated it. In our study, oxidative stress inhibited cell growth and induced significant G0/G1 phase arrest, accompanied by increased ANGPTL4 expression. Following GQZ-DS intervention, the proportion of cells in the G0/G1 phase decreased, and ANGPTL4 expression was reduced. These results suggest that ANGPTL4 may be associated not only with oxidative stress itself, but also with oxidative stress-related impairment of cell cycle progression.

4.3 Mechanisms of GQZ-DS-mediated attenuation of cellular oxidative injury

The pharmacological properties of GQZ-DS are consistent with the protective effects observed in the present study. In TCM, retinal degeneration is generally considered to involve both root deficiency and branch excess. The root deficiency primarily refers to insufficiency of the liver, kidney, Qi, and blood, whereas the branch excess is characterized by stagnation of the ocular collaterals. GQZ is believed to nourish the liver and kidney, thereby treating the root of the disease, while DS promotes blood circulation and removes blood stasis, addressing the secondary pathological manifestations. This combination embodies the therapeutic principle of tonifying deficiency and promoting blood circulation. Modern pharmacological studies support this rationale. GQZ exhibits potent antioxidant activity, reduces retinal ROS levels, and inhibits photoreceptor apoptosis [28]. DS improves blood flow and alleviates blood stasis-related injury [29]. Salvianolic acid A attenuates H_2O_2-induced endothelial oxidative damage through a mechanism involving miR-204-5p [30], whereas tanshinone IIA inhibited oxidative stress by regulating PI3K/AKT and Nrf2/HO-1 signaling pathways [31, 32]. Furthermore, previous study also showed that the GQZ-DS combination significantly increased SOD activity and reduced MDA levels [13], suggesting that GQZ-DS may inhibit oxidative injury through coordinated multi-component actions.

4.4 Limitations and future prospects

This study has several limitations that warrant consideration. First, the in vitro models employed, while useful for mechanistic dissection, lack the complex cellular interactions, microenvironmental cues, and systemic factors inherent to intact organisms, which could significantly modulate the observed responses. Second, regarding the herbal formulation investigated, which comprises multiple bioactive constituents, it remains challenging to attribute the observed effects to any individual component or to delineate potential synergistic, additive, or antagonistic interactions among them. Finally, as an upstream factor, how ANGPTL4 mediates the modulation of downstream molecular responses and whether it directly interacts with specific components of GQZ-DS remain to be investigated. Future studies should employ pathway intervention strategies to systematically elucidate the pharmacological mechanisms underlying GQZ-DS.

5 Conclusion

GQZ-DS effectively protected 661W retinal photoreceptor cells against H_2O_2-induced oxidative injury, as reflected by reduced oxidative stress, improved antioxidant

activity, alleviated cell cycle arrest, and decreased apoptosis. ANGPTL4 was identified as a functional mediator of oxidative injury, and its downregulation contributed to the protective effects of GQZ-DS. These results provide experimental support for the use of GQZ-DS in photoreceptor protection and suggest that targeting ANGPTL4-related signaling may represent a potential strategy for retinal degenerative diseases associated with oxidative stress.

Fundings

Natural Science Foundation of Hunan Province, China (2025JJ90027), Health Research Project of Hunan Provincial Health Commission (20255027), and Innovative Training Program for College Students of Hunan University of Chinese Medicine (205).

Author contributions

Jun Peng: conceptualization, methodology, data curation, and writing – original draft. Junjiang Jiang: methodology, methodology, formal analysis, and writing – original draft. Junnan Zhong: formal analysis and writing – original draft. Siyi Zhou: formal analysis and methodology. Tingyan Hu: methodology and visualization. Xuyu Chen: Methodology. Qinghua Peng: investigation and supervision. Yasha Zhou: funding acquisition, supervision, and writing – review & editing. All authors approved the submission and take responsibility for this manuscript.

Competing interests

Qinghua Peng is an editorial board member for *Digital Chinese Medicine* and was not involved in the editorial review or the decision to publish this article. All authors declare that there are no competing interests.

References

[1] WANG CY, YANG RY, SHAO Y, et al. Study on the mechanism of oxidative stress in ocular diseases and therapeutic strategies. Recent Advances in Ophthalmology, 2025, 45(3): 247–252.

[2] XIANG QC. Functional study of Mettl3 in retinal photoreceptor. Chengdu: University of Electronic Science and Technology of China, 2024.

[3] XU J, YANG YJ, QIN GY, et al. Effects of Lycii Fructus and Salviae Miltiorrhizae on the syndrome of deficiency with blood stasis in RCS (rdy-/-, p-/-) rats with retinitis pigmentosa: an intervention study. Digital Chinese Medicine, 2019, 2(3): 157–165.

[4] JIANG PF, OU C, PENG J, et al. Effects of Buxu Huoxue Method on expression of Caspase-12 precursor and Caspase-2 mature in retina of rd10 mice. China Journal of Traditional Chinese Medicine and Pharmacy, 2022, 37(1): 174–177.

[5] SONG HP, OU C, XIONG M, et al. Experimental study on treatment of retinitis pigmentosa by inducing Müller cell reprogramming with Lycii Fructus and Salviae Miltiorrhizae Radix et Rhizoma. China Journal of Chinese Materia Medica, 2024, 49(11): 3040–3049.

[6] CHENG RY, SONG WN, JIANG X, et al. Application of Lycii Fructus and its compound formulas in central nervous system diseases: a review. Chinese Journal of Experimental Traditional Medical Formulae, 2025, 31(22): 273–281.

[7] HUANG SH, LIU XY, LIU YX, et al. Research of progress on polysaccharides in TCM for treatment alcoholic liver injury. China Journal of Chinese Materia Medica, 2026, 51(3): 610–622.

[8] SONG WN, ZHANG SX, LU F, et al. Active components of Salviae Miltiorrhizae Radix et Rhizoma and its compound in treatment of nervous system diseases: a review. Chinese Journal of Experimental Traditional Medical Formulae, 2025, 31(2): 303–313.

[9] QI Y, ZHOU CQ, CHEN B. Transcriptome combined single-cell sequencing explores molecular mechanisms of ANGPTL4 in sepsis-induced acute lung injury. PLoS One, 2025, 20(7): e0328551.

[10] ZHENG ZY, CAO PF, CHEN WQ, et al. The role and mechanism of ANGPTL4. Chemistry of Life, 2024, 44(5): 890–899.

[11] QIN Y, DINABANDHU A, CAO X, et al. ANGPTL4 influences the therapeutic response of patients with neovascular age-related macular degeneration by promoting choroidal neovascularization. JCI Insight, 2022, 7(13): e157896.

[12] YANG XY, CHENG Y, SU GF. A review of the multifunctionality of angiopoietin-like 4 in eye disease. Bioscience Reports, 2018, 38(5): BSR20180557.

[13] YANG YJ, WANG Y, DENG Y, et al. Fructus Lycii and Salvia Miltiorrhiza Bunge extract attenuate oxidative stress-induced photoreceptor ferroptosis in retinitis pigmentosa. Biomedicine & Pharmacotherapy, 2023, 167: 115547.

[14] FERNÁNDEZ-HERNANDO C, SUÁREZ Y. ANGPTL4: a multifunctional protein involved in metabolism and vascular homeostasis. Current Opinion in Hematology, 2020, 27(3): 206–213.

[15] WANG YQ, LU JL, CARISEY AF, et al. Innate immune and metabolic signals induce mitochondria-dependent membrane lysis via mitoxyperiosis. Cell, 2025, 188(25): 7155–7174.

[16] ARYAL B, ROTLLAN N, ARALDI E, et al. ANGPTL4 deficiency in haematopoietic cells promotes monocyte expansion and atherosclerosis progression. Nature Communications, 2016, 7: 12313.

[17] MCGARRY T, BINIECKA M, VEALE DJ, et al. Hypoxia, oxidative stress and inflammation. Free Radical Biology and Medicine, 2018, 125: 15–24.

[18] SANTULLI G. Angiopoietin-like proteins: a comprehensive look. Frontiers in Endocrinology, 2014, 5: 4.

[19] TIAN Z, ZHANG TT, LI J. Research progress of microRNA in oxidative stress and lipid metabolism of non-exudative age-related macular degeneration. International Eye Science, 2024, 24(4): 561–566.

[20] WANG S, LIU SQ. Effects of ubiqutin-proteasome system in retinopathy and their mechanism. Chinese Journal of Experimental Ophthalmology, 2019, 37(10): 843–848.

[21] TONADE D, LIU HT, KERN TS. Photoreceptor cells produce inflammatory mediators that contribute to endothelial cell death in diabetes. Investigative Opthalmology & Visual Science, 2016, 57(10): 4264.

[22] ZHANG SM, FAN B, LI YL, et al. Oxidative stress-involved mitophagy of retinal pigment epithelium and retinal degenerative diseases. Cellular and Molecular Neurobiology, 2023, 43(7): 3265–3276.

[23] LI P, WU J, LI J, et al. Correlation of the expression levels of ANGPTL4 and SDF-1 in serum with severity of disease in patients with diabetic macular edema. International Eye Science,

2025, 25(3): 461–464.
[24] YANG HL, YAO DP. Evaluation value of PDGF, MCP-1 and ANGPTL4 levels in aqueous humor for anti-VEGF therapeutic efficacy of neovascular glaucoma. International Journal of Laboratory Medicine, 2025, 46(12): 1455–1460.
[25] LI XM, TULAKE GZLNE. Relationship between levels of sICAM-1, sVEGFR-1, ANGPTL4 in aqueous humor and macular edema in patients with retinal vein occlusion and effects of ranibizumab therapy. Shandong Medical Journal, 2024, 64(1): 64–67.
[26] WANG N, LI HB, SUN QQ, et al. The exploration of disturbance of capillary and photoreceptor communication networks in diabetic retinopathy through single-cell RNA-seq. Journal of Cellular and Molecular Medicine, 2025, 29(5): e70442.
[27] WEN Y, ZHANG XF, LIU H, et al. SGLT2 inhibitor downregulates ANGPTL4 to mitigate pathological aging of cardiomyocytes induced by type 2 diabetes. Cardiovascular Diabetology, 2024, 23(1): 430.
[28] YANG YJ, WANG Y, DENG Y, et al. *Lycium barbarum* polysaccharides regulating miR-181/Bcl-2 decreased autophagy of retinal pigment epithelium with oxidative stress. Oxidative Medicine and Cellular Longevity, 2023, 2023: 9554457.
[29] SU CY, MING QL, RAHMAN K, et al. *Salvia miltiorrhiza*: traditional medicinal uses, chemistry, and pharmacology. Chinese Journal of Natural Medicines, 2015, 13(3): 163–182.
[30] QIAO XL, CAO SY, CHEN SY, et al. Salvianolic acid A alleviates H_2O_2-induced endothelial oxidative injury via miR-204-5p. Scientific Reports, 2024, 14: 11931.
[31] FANG M, HUANG DR, ZHANG JW, et al. Tanshinone IIA exerts anti-hepatocellular carcinoma effects by inhibitingoxidative stress via PI3K/AKT and Nrf2/HO-1 signaling pathway. China Journal of Chinese Materia Medica, 2024, 49(24): 6724.
[32] OU C, JIANG PF, TIAN Y, et al. Fructus Lycii and *Salvia miltiorrhiza* Bunge extract alleviate retinitis pigmentosa through Nrf2/HO-1 signaling pathway. Journal of Ethnopharmacology, 2021, 273: 113993.

(Editor-in-Charge Siyi Wei)

枸杞子-丹参调节 ANGPTL4 对视网膜感光细胞氧化损伤的改善作用

彭俊[a], 蒋俊将[b], 钟俊楠[b], 周思艺[b], 胡婷雁[b], 陈煦瑜[b], 彭清华[c], 周亚莎[b*]

a. 湖南中医药大学第一附属医院眼科, 湖南 长沙 410007, 中国
b. 湖南中医药大学中西医结合学院, 湖南 长沙 410208, 中国
c. 湖南中医药大学中医学院, 湖南 长沙 410208, 中国

【摘要】目的 研究枸杞子-丹参对过氧化氢（H_2O_2）诱导的 661W 视网膜感光细胞氧化损伤的保护作用，并探讨该作用是否与血管生成素样蛋白 4（ANGPTL4）相关。**方法** 采用液相色谱-质谱联用技术（LC-MS）对枸杞子-丹参水提液的主要成分进行鉴定，并通过 H_2O_2 处理 661W 细胞建立氧化损伤模型。采用细胞计数法（CCK-8）确定 H_2O_2 造模和枸杞子-丹参的干预浓度。细胞分别予以枸杞子-丹参、ANGPTL4 基因敲低或 ANGPTL4 过表达处理。通过流式细胞术检测细胞周期、细胞凋亡率及细胞内活性氧（ROS）水平；使用硫代巴比妥酸（TBA）比色法测定丙二醛（MDA）含量和超氧化物歧化酶（SOD）活性；采用免疫荧光法检测 ANGPTL4 蛋白表达；通过实时荧光逆转录聚合酶链式反应（RT-qPCR）测定 ANGPTL4 mRNA 的表达水平；采用蛋白质印迹法检测 ANGPTL4 和裂解型半胱氨酸天冬氨酸蛋白酶-3 的蛋白表达水平。**结果** LC-MS 鉴定出了枸杞子-丹参水提液的五种主要成分：2-O-β-D-吡喃葡萄糖基-L-抗坏血酸、芦丁、D-半乳糖、丹参酚酸 A 和丹参酮 IIA。CCK-8 筛选出 300 μmol/L 的 H_2O_2 用于诱导细胞的氧化应激损伤，0.05 g/mL 和 0.1 g/mL 作为低剂量和高剂量的枸杞子-丹参浓度用于后续实验。H_2O_2 处理导致 661W 细胞活性降低，ROS 和 MDA 表达水平升高，SOD 活性下降，凋亡率增加，裂解型半胱氨酸天冬氨酸蛋白酶-3 表达上调，以及细胞周期停滞于 G0/G1 期。枸杞子-丹参低剂量及高剂量治疗可缓解这些损伤变化，其中高剂量的枸杞子-丹参的缓解作用更显著（$P < 0.05$ 或 $P < 0.01$）。枸杞子-丹参还降低了 ANGPTL4 mRNA 水平和 ANGPTL4 蛋白水平。对细胞进一步进行质粒转染后发现，敲低 ANGPTL4 基因可减轻 661W 细胞的氧化应激损伤和凋亡，而 ANGPTL4 过表达则加剧了损伤和凋亡。此外，枸杞子-丹参可部分逆转 ANGPTL4 过表达诱导的细胞氧化损伤。**结论** 枸杞子-丹参能减轻 H_2O_2 导致的 661W 视网膜光感受器细胞的氧化损伤，该作用与下调 ANGPTL4 的表达有关。

【关键词】枸杞子-丹参；视网膜感光细胞；血管生成素样蛋白 4；氧化损伤；细胞凋亡